IEEE Access
Multidisciplinary | Rapid Review | Open Access Journal

Received May 8, 2020, accepted May 20, 2020, date of publication May 26, 2020, date of current version June 10, 2020.

Digital Object Identifier 10.1109/ACCESS.2020.2997728

Online Estimation of Power System Inertia Constant Under Normal Operating Conditions

FANHONG ZENG[1], (Graduate Student Member, IEEE),
JUNBO ZHANG[1], (Senior Member, IEEE),
GE CHEN[1], (Graduate Student Member, IEEE),
ZIKUN WU[1], SIWEI HUANG[1], AND
YINGQI LIANG[2], (Member, IEEE)
[1]School of Electric Power, South China University of Technology, Guangzhou 510641, China
[2]Department of Electrical and Computer Engineering, National University of Singapore, Singapore 119077

Corresponding author: Junbo Zhang (epjbzhang@scut.edu.cn)

This work was supported in part by the National Natural Science Foundation of China under Grant 51761145106, in part by the Natural Science Foundation of Guangdong Province, China, under Grant 2018B030306041, and in part by the Fundamental Research Funds for the Central Universities under Grant 2019SJ01.

ABSTRACT An online estimation method for the power system inertia constant under normal operating conditions is proposed. First of all, a dynamic model relating the active power to the bus frequency at the generation node is identified in the frequency domain using ambient data measured with the phasor measurement units (PMUs). Then, the inertia constant at the generation node is extracted from the unit step response of the identified model in the time domain using the swing equation. Finally, with the sliding window method and the exponential smoothing method, the estimated inertia constant is updated in real-time. Compared to the conventional methods using large disturbance data or field test data, the proposed method can estimate the inertia constant under normal operating conditions, and therefore, can provide the tracking trajectory of the power system inertia constant in real-time. The effectiveness of the proposed method is validated in the IEEE 39-bus system. The results show that the relative error of the identified inertia constant is below 5% and the identified inertia constant can be updated within 1s.

INDEX TERMS Inertia constant estimation, ambient signals, subspace identification, step response, sliding window, exponential smoothing.

I. INTRODUCTION

In the point view of physics, the inertia of a power system is its capability to resist energy fluctuations caused by external disturbances, which, in conventional power systems, are supplied mainly by the kinetic energy stored in the rotating mass of the synchronous generators and quantified by the inertia constant [1].

With the increasing share of the power electronic inverter interfaced renewable energy sources (RESs), some changes have taken place in power system inertia. Many synchronous generators are displaced by RESs, thus leading to a persistent decrease in the conventionally available inertia resources [2]–[4]. Meanwhile, with different control strategies and parameters, various inertia suppliers such as virtual inertia control and energy storage systems are employed to improve the power system inertia [5]–[7]. Therefore, the power system inertia, as well as its quantification, not only decrease but also become time-varying [8].

In conventional power systems, the inertia constant is steady over the long term, and therefore, is chosen as a fundamental reference to the design of frequency stability controls and many of the protection relays [1]. When the penetration of RESs becomes higher, the situation is different. For instance, the system frequency may drop badly when the system suffers an active power deficiency, and consequently, the protection and control devices such as under-frequency load shedding or disconnection of generators may be triggered reluctantly [9]. Since there is no mature method to track the power system inertia in real-time, to avoid the malfunction of the protection relays and stability controllers, the transmission system operators (TSOs) must adopt more conservative operational schemes to ensure the stable operation of the power system, which inflates the power system operational costs.

The associate editor coordinating the review of this manuscript and approving it for publication was Lei Chen.

Given the issues mentioned above, the need for online estimation of power system inertia (constant) is highlighted and has drawn consistent attention in recent years. According to the measurement data types, the existing estimation methods can be categorized into two groups: 1) disturbance data methods, and 2) non-disturbance data methods.

For most of the estimation methods based on disturbance measurements, the inertia (constant) is estimated using the swing equation, utilizing post-event data that record the transient active power and frequency characteristics of the generators [10]–[21]. For instance, a procedure for estimating the total inertia of the Great Britain power system was proposed in [13], which calculated the total inertia for the whole system by summing all the estimated regional inertias. An online algorithm to estimate the system inertia after a disturbance based on sliding windows of active power and frequency derivative measurements was proposed in [14]. In [17], an inertia estimation method based on the extended Kalman filter was proposed, which needs to assume the time of disturbance. Based on the transient and steady state characteristics of the frequency response after a disturbance, a method to estimate the equivalent inertia and damping constant simultaneously was proposed in [18]. In [19], an approach for online inertia estimation in the power system network with solar photovoltaic source was proposed using the synchronized measurements from PMUs. In [20], based on the measured frequency response for any arbitrary disturbance in the system, a method to estimate the available inertia in an islanded microgrid was proposed. In addition, some other disturbance data methods have recently been developed. In [21], an approach based on electromechanical wave theory was presented to identify the change of power system inertia distribution. Though both the offline and online methods based on recorded disturbances can estimate the inertia accurately, they cannot achieve continuous inertia estimation as the natural transient events are deficient, and the transient field experiments are expensive.

Compared to the disturbance data methods, estimators based on non-disturbance measurements are quite limited. In [22], a statistical model-based real-time inertia estimation method was proposed, in which the model was trained to learn the features that relate the steady-state average frequency variations and the system inertia. In [23], ambient frequency and active power data were employed to estimate the effective inertia of a power system, where a combined model of inertial response and primary control was identified, and then the inertia was extracted from the impulse response of the model. However, the inertia tracking trajectory could not be provided in real-time in [23]. In our previous work, a closed-loop identification method was proposed for the power system equivalent inertia constant online estimation, which could achieve a precise estimation result, but it required the injection of an additional probing signal [24].

In this paper, we propose a more robust online estimation method for the power system inertia constant under normal operating conditions. Compared to the conventional methods based on transient test, probing and etc., the proposed method can achieve a precise inertia constant estimation without any disturbance event and probing injection, and can provide the tracking trajectory of the inertia constant in real-time. To our knowledge, it is the first work to track the inertia constant under normal operating conditions.

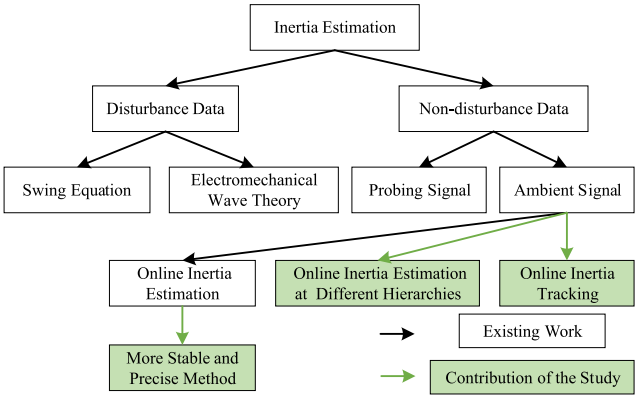

FIGURE 1. Contributions of the study to inertia estimation.

In relation to the existing work on inertia estimation, the contributions of this study are clarified in Fig. 1 and summarized as follows: 1) it provides a more stable and precise solution to identify power system inertia constant using ambient signals; 2) it realizes the estimation of inertia constant at different hierarchies (individual generator, area and the whole system) under normal operating conditions; 3) it realizes the real-time online tracking of inertia constant in the time scales of seconds under normal operating conditions, which can timely provide important information for stable operation of the power system.

The remainder of the paper is organized as follows: section II provides the theoretical fundamentals about power system inertia; section III introduces the proposed inertia constant online estimation method; section IV presents simulation results in the IEEE 39-bus system to verify the feasibility of the proposed method; section V concludes the paper.

II. THEORETICAL FUNDAMENTALS

A. INERTIAL RESPONSE AND INERTIA CONSTANT

After a disturbance, the frequency response of a traditional power system will sequentially go through three stages: the inertial response, the primary response and the secondary response [13]. During the inertial response, the rotating kinetic energy stored in the synchronous generators is released spontaneously to maintain the power balance, thus reducing the rate of change of frequency (RoCoF).

The rotational kinetic energy of a synchronous generator is usually normalized to an inertia constant, which is defined as the ratio of the stored rotational kinetic energy at the rated rotating speed to the rated capacity of the synchronous generator [1], namely:

$$H_i = \frac{E_i}{S_i} \tag{1}$$

where H_i is the inertia constant of generator i, E_i is the rotational kinetic energy of generator i and S_i is the rated capacity of generator i. Physically, H_i represents the time duration to supply energy for the demand that equals to the rated capacity of the generator, without any additional mechanical input.

In a power-electronics-dominated power system, the converter-interfaced RESs are initially inertia-free and the system frequency response does not have clear three-stages. However, virtual inertial response can be obtained with control of electrical converters, then converter-interfaced RESs can provide equivalent inertia for the power system. Besides, the dynamics of inertial response provided by converter-interfaced RESs can be described by a first-order differential equation [25], [26], which is similar to the swing equation of the synchronous generator. Namely, the inertial response of converter-interfaced RESs is mathematically equivalent to that of the synchronous generators [27]. Therefore, when estimating the equivalent inertia constant of the converter-interfaced RESs, it is reasonable to regard them as the equivalent synchronous generators and the proposed estimation method can be employed.

Further, in a multimachine power system, if we consider the other inertia contributors as the equivalent synchronous generators, then the equivalent inertia constant of the entire power system can be calculated as follows:

$$H_{sys} = \frac{1}{S_{sys}} \sum_{i=1}^{N} H_i S_i \tag{2}$$

where H_{sys} is the equivalent inertia constant of the system, S_{sys} is the rated capacity of the system and N is the number of generators.

B. SWING EQUATION

The dynamics between active power and frequency of a synchronous generator in a short time frame after a power mismatch can be modeled by the swing equation. For synchronous generator i, considering the damping effects, the swing equation can be written as [1]

$$\dot{f}_{r,i} = \frac{1}{2H_i}(P_{m,i} - P_{e,i} - D_i \Delta f_{r,i}) \tag{3}$$

where $P_{m,i}$ and $P_{e,i}$ are the mechanical power (in p.u.) and the electrical power (in p.u.) of generator i, respectively; $f_{r,i}$ is the rotor electrical frequency (in p.u.) of generator i; and D_i is the damping coefficient of generator i. Physically, when suffering a power mismatch, the RoCoF of the synchronous generator is constrained by the inertia constant and the damping coefficient in a short time frame, thus the frequency of the generator cannot change suddenly and the frequency stability can be improved.

As an approximation, the dynamic behavior of a certain area or the system can be represented as an equivalent synchronous generator j, which leads to the aggregated swing equation as follows:

$$\dot{f}_j = \frac{1}{2H_j}(P_{m,j} - P_{e,j} - D_j \Delta f_j) \tag{4}$$

where $P_{m,j}$ and $P_{e,j}$ denotes the total mechanical power and the total electrical power of the area or the system (in p.u.), respectively; f_j denotes the aggregated frequency of the area or the system (in p.u.); H_j denotes the equivalent inertia constant of the area or the system; and D_j denotes the total damping coefficient of the area or the system. The theoretical value of H_j can be calculated using (2).

Under normal operating conditions, all the variables in (3) vary around the steady-state operating point. Therefore, formula (3) can be written as the incremental formulation around the steady-state operating point as follows:

$$\Delta\dot{f}_{r,i} = \frac{1}{2H_i}(\Delta P_{m,i} - \Delta P_{e,i} - D_i \Delta f_{r,i}) \tag{5}$$

Assuming $\Delta P_{m,i}$ to be zero and taking the Laplace transform on both sides of (5), we can reformulate the swing equation as a first-order transfer function:

$$G_i(s) = \frac{\Delta f_{r,i}(s)}{\Delta P_{e,i}(s)} \approx -\frac{1}{2H_i s + D_i} \tag{6}$$

where $\Delta f_{r,i}$ represents the rotor electrical frequency deviation of generator i, $\Delta P_{e,i}$ represents the electrical power deviation of generator i, and $G_i(s)$ (s is the Laplace operator) is the transfer function from $\Delta P_{e,i}$ to $\Delta f_{r,i}$, which is characterized by H_i and D_i. Besides, the transfer function from $\Delta P_{e,j}$ to Δf_j is similar to that in (6), which is characterized by H_j and D_j.

III. METHODOLOGY

The methodology proposed in this paper is for power system inertia constant real-time online estimation under normal operating conditions, which is shown in Fig.2. The key procedures include signal selection and preprocessing, system identification, inertia constant extraction and inertia constant tracking. All the key procedures can be realized automatically with low computational burden, and their details are expanded in the following subsections.

A. SIGNAL SELECTION AND PREPROCESSING

According to section II-B, the dynamic model of generator i can be identified using electrical power $P_{e,i}$ as the input and rotor electrical frequency $f_{r,i}$ as the output. However, $P_{e,i}$ and $f_{r,i}$ in the real power system are difficult to measure. As a substitute, $P_{e,i}$ and $f_{r,i}$ can be approximated by the active power output P_i and the frequency f_i at the generator connection bus, respectively. In practice, P_i and f_i can be measured by PMUs installed at the generator connection bus. Therefore, we can identify the dynamic model of generator i using active power output P_i as the input and bus frequency f_i as the output. Namely, the following equation holds:

$$G_i(s) \approx \frac{\Delta f_i(s)}{\Delta P_i(s)} \approx -\frac{1}{2H_i s + D_i} \tag{7}$$

Additionally, it is possible to identify the dynamic model of a certain area (or the system) using the total active power output and the aggregated frequency of the area (or the system) as input and output, respectively. It would be simple

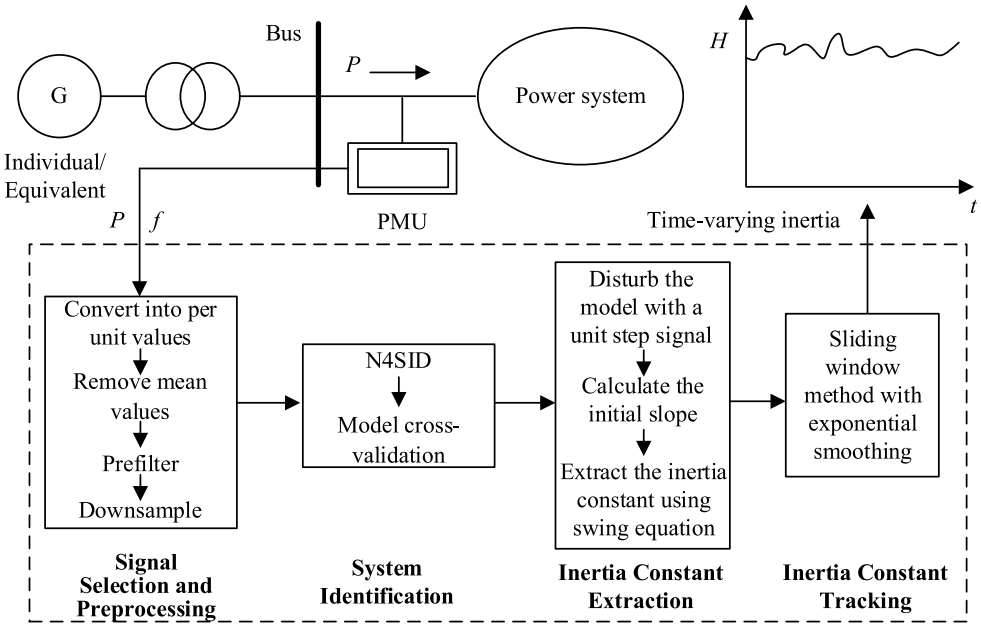

FIGURE 2. Flow chart of the proposed methodology.

to obtain the total active power output by summing up all active power outputs in the area (or the system). To aggregate the frequency, however, the center of the inertia frequency is commonly used, which is an average frequency weighted by the inertia of each node and cannot be measured directly [23].

Here we propose a simplified aggregated frequency to represent the center of inertia frequency. The frequency of the area (or the system) is evaluated by a weighted average of the measured frequencies as follows:

$$f_j = \frac{\sum_{i=1}^{i=N_j} w_i f_i}{\sum_{i=1}^{i=N_j} w_i} \tag{8}$$

where f_i denotes the frequency at the generator connection bus, and N_j denotes the number of online generators in the area (or the system). Here, the weights w_i are determined based on the following consideration: the larger the inertia constant of generator i, the smaller the variations of the bus frequency f_i under normal operating conditions. Therefore, the weights w_i are defined as the inverse of the variance of bus frequency f_i, namely, $w_i = 1/\mathrm{var}(f_i)$.

Under normal operating conditions, the ambient data measured by PMUs are commonly polluted with noise, so signal preprocessing is a necessary procedure to improve identification efficiency and accuracy before running an identification algorithm [28], [29]. First, all the signals are converted into per unit values by dividing their base values. Then, all the signals are detrended by removing their mean values and prefiltered using a noncausal Butterworth low-pass filter. As the typical values for H_i are in the range of 2-10 s [1], a noncausal Butterworth low-pass filter with a 0.5 Hz cut-off frequency is suitable to attenuate the higher frequency components that can impair the inertia constant estimation. Finally, the signals are downsampled to the range of 5-10 Hz to avoid the numerical problems when running the identification algorithm.

B. SYSTEM IDENTIFICATION

Generally, the power system is nonlinear. However, under normal operating conditions, the disturbance to the power system is small, so the nonlinear power system can be approximated by a linear state space model around the steady-state operating point. An n^{th} other multi-input-multi-output state space model can be described as follows:

$$\begin{aligned} \boldsymbol{x}_{k+1} &= \boldsymbol{A}\boldsymbol{x}_k + \boldsymbol{B}\boldsymbol{u}_k + \boldsymbol{\omega}_k \\ \boldsymbol{y}_k &= \boldsymbol{C}\boldsymbol{x}_k + \boldsymbol{D}\boldsymbol{u}_k + \boldsymbol{v}_k \end{aligned} \tag{9}$$

where $\boldsymbol{x}_k \in R^n$ is the state vector; $\boldsymbol{u}_k \in R^m$ is the input vector; $\boldsymbol{y}_k \in R^l$ is the output vector; and $\boldsymbol{A} \in R^{n\times n}$, $\boldsymbol{B} \in R^{n\times m}$, $\boldsymbol{C} \in R^{l\times n}$, and $\boldsymbol{D} \in R^{l\times m}$ are system matrixes to be identified. Additionally, ω_k and v_k denote random sequences of process noises and measurement noises, respectively.

Subspace identification methods are effective algorithms to identify the state space model with ambient data and can be implemented in different ways [30]. As a widely used algorithm in subspace identification [28], the N4SID (Numerical algorithm for Subspace State Space System IDentification) algorithm is used in this paper. The main feature of the N4SID algorithm is to calculate matrix $\Gamma_{\mathbf{k}}$ through oblique projection as follows:

$$\boldsymbol{\Gamma}_k = \left(\boldsymbol{Y}_f \middle| \begin{bmatrix} \boldsymbol{U}_p \\ \boldsymbol{Y}_p \end{bmatrix}\right) / \boldsymbol{U}_f \tag{10}$$

where / denotes the oblique projection. Then, singular value decomposition (SVD) is applied on $\boldsymbol{\Gamma}_{\mathrm{k}}$ to determine the order

of the identified model. Specifically, the order of the identified model is equal to the number of the dominant singular values of matrix $\boldsymbol{\Gamma}_k$. The SVD can be partitioned into the following form:

$$\boldsymbol{W}_1\boldsymbol{\Gamma}_k\boldsymbol{W}_2 = \begin{bmatrix}\boldsymbol{U}_1 & \boldsymbol{U}_2\end{bmatrix}\begin{bmatrix}\boldsymbol{S}_1 & \boldsymbol{0}\\ \boldsymbol{0} & \boldsymbol{S}_2\end{bmatrix}\begin{bmatrix}\boldsymbol{V}_1^T\\ \boldsymbol{V}_2^T\end{bmatrix} \approx \boldsymbol{U}_1\boldsymbol{S}_1\boldsymbol{V}_1^T \tag{11}$$

where $\boldsymbol{W}_1$ and $\boldsymbol{W}_2$ are the identity weighing matrixes. In (11), the insignificant singular values are neglected by removing $\boldsymbol{S}_2$ as the dominant singular values determine the main dynamics of the system. Finally, the system matrixes $\boldsymbol{A}$, $\boldsymbol{B}$, $\boldsymbol{C}$ and $\boldsymbol{D}$ can be obtained by solving the linear equations. Readers can refer to [28] for the details of the N4SID algorithm.

Generally, the order of the real system is rather high as it contains many complicated control systems. However, a model with a lower order is identified in this part. Though the order of the identified model is lower than the order of the real power system, it is accurate enough to capture the dynamics of the inertial response. The N4SID algorithm can search the best order for the identified model automatically after setting a range of orders from $n_{\min}$ to $n_{\max}$. Empirically, $n_{\min}$ can be set as 1 and $n_{\max}$ can be set as 10 for inertia constant estimation.

After running the identification algorithm, the reliability of the identified model should be verified by model cross-validation. The model cross-validation can be performed by comparing the validated output $\hat{y}(t)$ and the original output $y(t)$. To evaluate the reliability of the identified model quantitatively, the fitting ratio (FR) between the validated output $\hat{y}(t)$ and original output $y(t)$ is defined as follows:

$$FR = \left(1 - \frac{\sum_{t=1}^{N}(\hat{y}(t) - y(t))^2}{\sum_{t=1}^{N} y(t)^2}\right) \times 100\% \tag{12}$$

where N is the number of samples.

C. INERTIA CONSTANT EXTRACTION

Theoretically, the state space model includes the inertia constant but as an implicit value, so further analysis should be employed for the identified model. A direct way is to extract the inertia constant from the model itself in the frequency domain after some transformation. First, the state space model can be transformed into a transfer function from ΔP_i to Δf_i. Then, the transfer function is reduced to a first order inertia function the same as (7) and finally, the inertia constant H_i is estimated together with D_i. However, large error may be introduced during the order reduction process, leading to inaccurate estimation of the inertia constant. For this reason, we propose a method to extract the inertia constant from the step response of the identified model in the time domain.

According to section III-B, the real power system can be approximated by a linear model and the model is reliable if the model cross-validation performs well. In other words, the identified model can be regarded as the real power system model to some extent. In this perspective, when a certain disturbance is applied to the identified model, the disturbance source can be regarded as the active power deviation ΔP_i and the corresponding response can be regarded as the bus frequency deviation Δf_i.

If we disturb $G_i(s)$ with an unit step signal, namely, $\Delta P_i = -\varepsilon(t)$ ($\varepsilon(t)$ is the unit step function), then Δf_i can be expressed as (13) in Laplace domain.

$$\Delta f_i(s) = \frac{1}{2H_i s + D_i}\frac{1}{s} \tag{13}$$

The equation can be solved directly and be written as follows in the time domain:

$$\Delta f_i(t) = \frac{1}{D_i}(1 - e^{-\frac{D_i}{2H_i}t}) \tag{14}$$

Then the slope of the unit step response at $t = 0$ can be calculated as:

$$\Delta\dot{f}_i\,|_{t=0} = \frac{1}{2H_i} \tag{15}$$

According to (15), the inertia constant H_i is determined by the initial RoCoF $\Delta\dot{f}_i\,|_{t=0}$, namely the initial slope of the unit step response of $G_i(s)$. Therefore, we can disturb the identified model with a unit step signal and calculate the initial slope of the corresponding response as $\Delta\dot{f}_i\,|_{t=0}$. The problem turns into how to estimate $\Delta\dot{f}_i\,|_{t=0}$ after the disturbance as accurate as possible. As the inertial response activates immediately after the disturbance and lasts a short time, we recommend calculating $\Delta\dot{f}_i\,|_{t=0}$ with a 500 ms sample-by-sample sliding window[1] over 1-2 s period [13] from the unit step response of the identified model. For power systems of various sizes, the data length of the unit step response for the $\Delta\dot{f}_i\,|_{t=0}$ calculation can be adjusted properly according to the dynamics of the systems. During each sliding window, $\Delta\dot{f}_i\,|_{t=0}$ is estimated as the slope of a linear fit to the response. The maximum slope is then taken to represent the $\Delta\dot{f}_i\,|_{t=0}$ during the inertial response period following the disturbance.

Note that, the discrete time identified model should be converted into continuous time model before evaluating step response. Then, the continuous time model should be checked for stability in s-domain, namely, the real part of poles should be less than zero. The functions *d2c*, *step*, *polyfit* in MATLAB can be used in this part for inertia constant extraction.

The proposed RoCoF calculation method is also applicable for the event data of real power systems. In other words, the inertia constant can be estimated from the event data based on the proposed RoCoF calculation method and the swing equation. In this case, the event data can be treated as a complementary of ambient data.

D. INERTIA CONSTANT TRACKING

In this part, sliding window[2] method and exponential smoothing method are used to update the estimated results in real-time, thus realizing the online tracking of the inertia constant.

[1,2] The sliding windows in these two parts are different. The former is for RoCoF calculation, and the latter is for inertia constant tracking.

For the sliding window method, a fixed size time window is used to estimate the inertia constant, and the window is gradually updated for the next estimation. The performance of the sliding window method is dependent on both the choice of sliding window length and the estimation refresh rate.

Generally, the estimation accuracy increases with sliding window length. However, no estimates are available during the first sliding window, and the time delay of the first estimation result can be reduced with a shorter sliding window length. The estimation refresh rate determines how fast a new estimation should be done. Though a faster refresh rate makes the estimator more responsive for real-time estimation as well as tracks change of inertia constant better, it increases computational burden, thus leading to a longer execution time.

Though the inertia constant extracted from the identified models can be updated in real-time, there may be a few low *FR* models that introduce inaccurate estimates, leading to large fluctuations of the inertia constant. To smooth the estimates from the low *FR* models, the exponential smoothing method was used, whose original form is defined as:

$$v_t = \alpha\theta_t + (1-\alpha)v_{t-1} \tag{16}$$

where v_t and v_{t-1} are the smoothing value at time t and time $t-1$, respectively; θ_t is the actual value at time t; and α is the smoothing constant, ranging from 0 to 1.

In addition, the inertia constant extracted from the unstable identified model is far from the real value, which should be detected and removed. In this paper, we replace the abnormal estimates from the unstable identified model at time t with the estimates at time $t-1$.

Combining the methods mentioned above, the inertia constant can be updated as follows:

$$H_t = \begin{cases} \mu_t^k h_t + (1-\mu_t^k)H_{t-1}, & \textit{if stable} \\ H_{t-1}, & \textit{if unstable} \end{cases} \tag{17}$$

where H_t and H_{t-1} are the smoothing value of inertia constant at time t and time $t-1$, respectively; h_t is the inertia constant extracted from the identified model at time t; μ_t is the fitting coefficient at time t, which is equal to *FR* divided by 100; and k is the exponent, which can be set from 20 to 80 to get a good smoothing effect.

IV. CASE STUDY

A. SYSTEM BACKGROUND

The proposed method was tested in the IEEE 39-bus system, which is a simplified model of high voltage transmission system in the northeast of the USA (New England area). The system consists of 10 generators, 39 buses, 19 loads, 34 lines and 12 transformers. The rated frequency is 60 Hz and the main voltage level is 345 kV. Generator 1 is the equivalent generator for the external power grid, and generator 2 is the balance generator. Automatic voltage regulators and governors are used for generator 2-10. The time domain simulations are carried out using Digsilent/ Powerfactory software. The single line diagram of the test system is shown in Fig. 3.

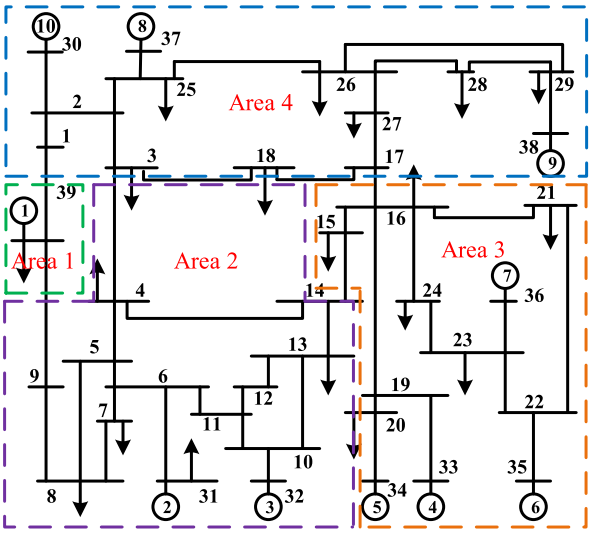

FIGURE 3. Single line diagram of the IEEE 39-bus system [31].

B. ONLINE INERTIA CONSTANT ESTIMATION

In this part, the inertia constant estimation accuracy of the proposed method is validated in the widely used IEEE 39-bus system mentioned above. All 19 loads in the 39-bus system are injected with Gaussian noise filtered by a low-pass filter with a cut-off frequency of 5 Hz, thus simulating the small random load fluctuations and other related small variations of real power systems during normal operating conditions. Then, the inertia constant of all the individual generators as well as the equivalent inertia constant of both the areas and the whole system is estimated using the methods introduced in section III-A to C.

1) ONLINE INERTIA CONSTANT ESTIMATION OF THE INDIVIDUAL GENERATOR

The experiment of a single estimation can be carried out with the following procedures:

Step 1: The bus frequency f_i at the generator connection bus and the active power output P_i are measured by PMUs. The length of the measurements is 200 s and the sampling rate is 100 Hz. The first 100 s signals are used for model identification, and the last 100 s signals are used for model cross-validation.

Step 2: Data preprocessing is employed to the signals. The bus frequency f_i and the active power output P_i are converted into per unit values by dividing their base values 60 Hz and 100 MW, respectively; the trend is removed; the high-frequency components are filtered using a noncausal low-pass filter with a cut-off frequency of 0.5 Hz; and the sampling rate is decreased from 100 Hz to 5 Hz to avoid numerical unstable problems.

Fig. 4 shows the preprocessed active power and bus frequency of generator 2. The fluctuations of both the active power and the bus frequency under normal operating conditions is rather small. The preprocessed measurements of other

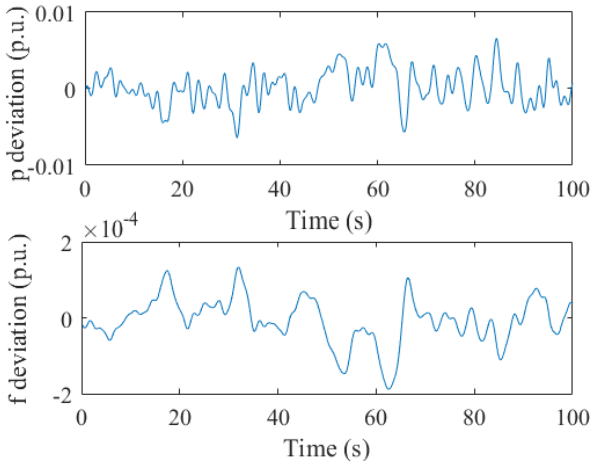

FIGURE 4. Preprocessed measurements of generator 2.

generators are not provided here since they are similar to that in Fig. 4.

Step 3: With the processed active power P_i and bus frequency f_i, the state space model with P_i as input and f_i as output is identified using N4SID. Then the model cross-validation is carried out to evaluate the reliability of the identified model.

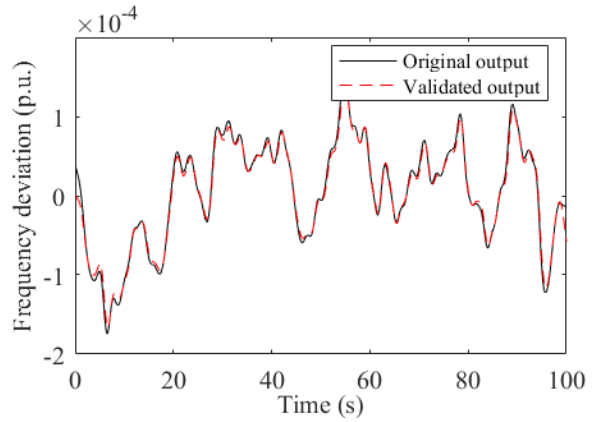

FIGURE 5. Model cross-validation result of generator 2.

Fig. 5 shows the model cross-validation result of generator 2. The model cross-validation results of other generators are not provided here since they are similar to that in Fig. 5. It indicates a reliable model is identified as the validated output fits the original output well.

Step 4: The inertia constant of the generator is extracted from the identified model using the method proposed in section III-C. The identified model is disturbed with a unit step signal; the unit step response of the identified model is collected; the initial RoCoF is calculated from the unit step response of the identified model; and the inertia constant is extracted using (15).

Fig. 6 shows the unit step response of the identified model of generator 2 as well as the calculation of initial RoCoF

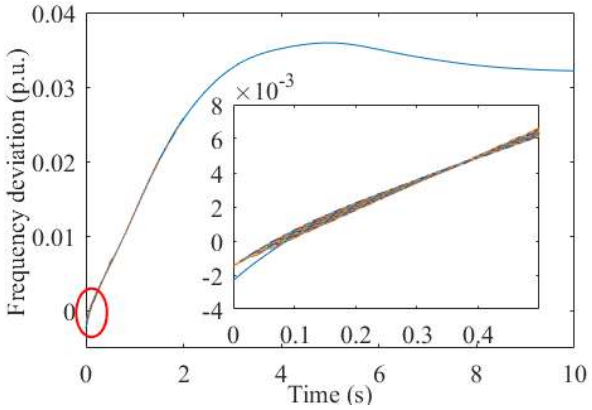

FIGURE 6. Calculation of the initial RoCoF during inertial response.

TABLE 1. Estimated inertia constant of all generators.

Generator	Bus	Order	H_{ref}	H_{est}	Error (%)
G01	39	5	500	506.06	1.21
G02	31	7	30.3	30.96	2.18
G03	32	7	35.8	36.42	1.73
G04	33	6	28.6	29.34	2.59
G05	34	7	26.0	25.40	-2.31
G06	35	5	34.8	34.99	0.55
G07	36	7	26.4	27.49	4.13
G08	37	5	24.3	23.61	-2.84
G09	38	7	34.5	35.93	4.14
G10	30	5	42	43.56	3.71

during inertial response, where the first 0.5 s of the result is enlarged. Table 1 shows the detailed results of the inertia constant estimation with a rated apparent power (S_b) of 100 MW. In Table 1, the estimated inertia constant (H_{est}) is very close to the real inertia constant (H_{ref}), and the largest relative error for the estimated inertia constant (H_{est}) is below 5%, thus the feasibility of the proposed method to estimate inertia constant of individual generator is verified.

Generally, the results from a single estimation are uncertain. To evaluate the accuracy of the proposed method and to further reduce the relative error by averaging the results from multiple estimations, the sliding window method is used to obtain various estimated results from one measurement period. In our simulations, a 10-minute measurement with a window length of 200 s and a refresh rate of 1 s is used; in total, 401 inertia constant estimations are carried out. For each estimation, steps 1-4 are employed sequentially; then, all the estimated results are obtained. After all of the estimations are completed, the results from the identified model with an *FR* above 95% are selected for statistical analysis, which means the point estimation and the 95% confidence interval (*CI*) estimation are carried out.

Fig. 7 shows the normal distribution behavior of the estimated inertia constant (H_{est}) of generator 2. It can see that 106 inertia constant estimates are selected for statistical analysis. The distribution of the estimated inertia constant from other generators is not provided here due to the limited space. Table 2 shows the statistical analysis results of the estimated inertia constant. In Table 2, we can see that the average of the

TABLE 2. Statistical analysis results of the estimated inertia constant.

Generator	H_{ref}	H_{avg}	ρ_H	H_{avg} *CI*-95%	ρ_H *CI*-95%	Error (%)
G01	500	510.01	29.61	498.73-521.28	20.50-40.06	2.00
G02	30.3	30.87	2.86	29.86-31.89	2.30-3.78	1.88
G03	35.8	36.24	3.25	35.67-36.81	2.89-3.71	1.23
G04	28.6	29.10	2.29	28.56-29.65	1.96-2.74	1.75
G05	26.0	26.54	1.52	25.97-27.10	1.21-2.04	2.08
G06	34.8	35.47	2.89	33.87-37.07	2.12-4.56	1.93
G07	26.4	26.90	1.99	26.00-27.81	1.52-2.87	1.89
G08	24.3	24.40	1.56	24.16-24.63	1.41-1.74	0.41
G09	34.5	35.02	2.13	33.77-35.08	1.75-2.70	1.51
G10	42	42.05	3.34	41.27-42.82	2.87-3.98	0.12

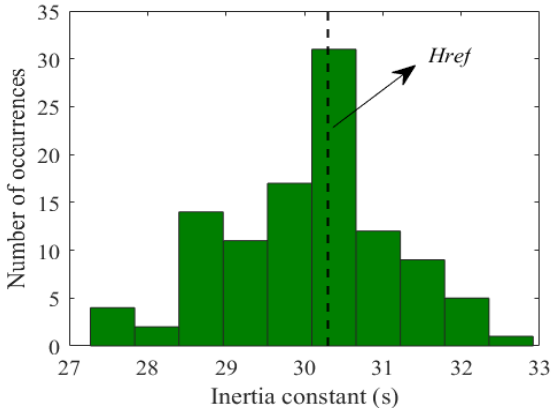

FIGURE 7. Distribution of the estimated inertia constant of generator 2.

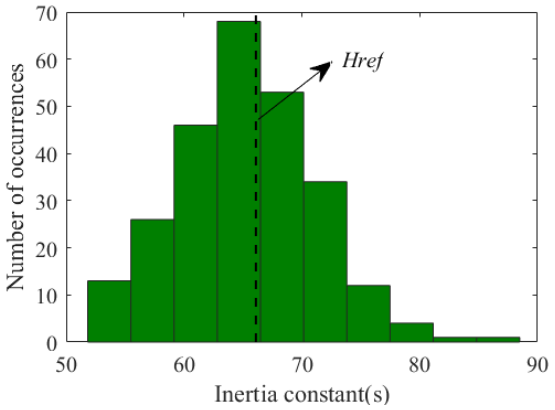

FIGURE 8. Distribution of the estimated inertia constant of area 2.

estimated inertia constant (H_{avg}) is nearly the same as the real inertia constant (H_{ref}), and all the real inertia constant (H_{ref}) values lie in the 95% *CI*. The variance of the estimated inertia constant (ρ_H) is rather small, meaning that the estimated values (H_{est}) fluctuate around the real values (H_{ref}) in a small range. Further, the relative error of all the estimated inertia constants is approximately 2%, which is less than the results of a single estimation, indicating sufficiently good performance of the proposed method.

2) ONLINE EQUIVALENT INERTIA CONSTANT ESTIMATION OF THE AREA AND THE WHOLE SYSTEM

Considering the coherence of the generators after a large disturbance, the 39-bus system can be divided into 4 areas, as shown in Fig. 2 [32]. Then, the equivalent inertia constant of the area and the whole system is estimated following steps 1 to 4. Note that the equivalent inertia constant of the area and the whole system is estimated by summing the active power outputs and aggregating the bus frequencies.

To evaluate the accuracy of the developed method and to further reduce the relative error, the sliding window method is used to obtain various estimates from one measurement period. In our simulations, a 10-minute measurement with a window length of 200 s and a refresh rate of 1 s is used; in total, 401 inertia constant estimations are carried out. In each estimation, steps 1 to 4 mentioned above are employed sequentially. After all of the estimations are completed, the results from the identified model with an *FR* above 95% are selected for statistical analysis.

Fig. 8 shows the normal distribution behavior of the estimated inertia constant (H_{est}) of area 2. It can see that 258 inertia constant estimates are selected for statistical analysis. The distribution of the estimates from other areas is not shown here because of space considerations. Table 3 shows the statistical analysis results for the estimations. In Table 3, we can find out that the average of the estimated inertia constant (H_{avg}) is nearly the same as the real inertia constant (H_{ref}), and all of the real inertia constant (H_{ref}) values are in 95% *CI*. The variance of the estimated inertia constant (ρ_H) is small, indicating the estimated values (H_{est}) narrowly fluctuate around the real values (H_{ref}). Further, the relative errors of all the estimated values are below 5%, thus verifying the effectiveness of the proposed method for estimating the equivalent inertia constant of the area or the whole system.

3) COMPARISON WITH THE DISTURBANCE DATA METHOD

The disturbance data method in [13] is carried out to compare with the method proposed in this paper.

Step 1: The active power of Load 15 is increased from 320 MW to 1820MW suddenly, resulting in an active power deficiency in the system. In this case, the active power imbalance ΔP is equal to 15 (in p.u.).

Step 2: The transient frequency following this event is measured. A five-order low pass Butterworth filter with a cutoff frequency of 0.5 Hz is used to isolate the dominant system inertial response. The processed transient frequency is shown in Fig. 9.

TABLE 3. Statistical analysis results of the estimated inertia constant.

Area/System	H_{ref}	H_{avg}	ρ_H	H_{avg} *CI*-95%	ρ_H *CI*-95%	Error (%)
Area 1	500	510.01	29.61	498.73-521.28	20.50-40.06	2.00
Area 2	66.1	64.81	5.96	63.57-66.31	5.49-6.53	-1.95
Area 3	115.8	118.24	6.87	115.77-120.80	5.49-9.18	2.15
Area 4	100.8	104.43	2.29	103.25-105.63	1.70-3.48	3.60
System	782.7	757.94	32.96	724.57-791.30	30.82-35.42	-2.94

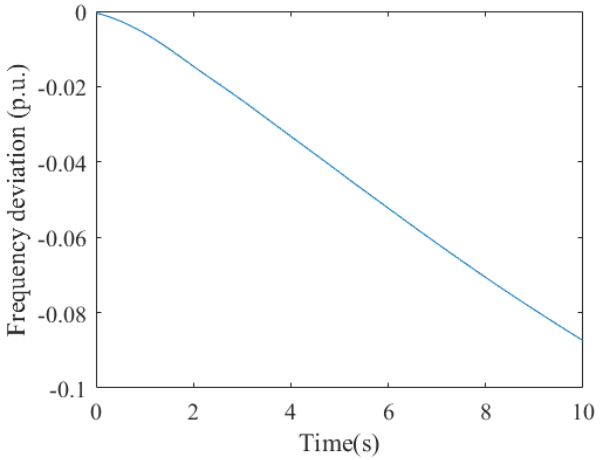

FIGURE 9. Preprocessed transient frequency measurement.

Step 3: The RoCoF is calculated using a 500-ms sample-by-sample sliding window, over a 2 s period following the event. The maximum value is then taken to represent the RoCoF following the event before the primary frequency response starts to take effect.

Step 4: With the method in [13], the equivalent inertia constant of the whole system is estimated as 809.98 s. The estimate value is close to the real value of 782.7 s and the relative error is 3.49%.

Besides, the relative error of the estimated inertia constant from the disturbance data method and that from the method proposed in this paper are both below 5%, thus verifying the effectiveness of the proposed method further.

C. ONLINE INERTIA CONSTANT TRACKING

In this part, the inertia constant online tracking capability of the proposed method is validated in the IEEE 39-bus system. Here, each synchronous generator of the 39-bus system is regarded as an equivalent generator, which is aggregated by all the generators of a certain area. The inertia constant of the synchronous generator of the 39-bus system is changed to simulate the time-varying equivalent inertia constant caused by the switching of the generators in the area. Considering a measurement length of 120 min, the inertia constant of all generators remains at H_1 during the first 40 min, then changes to H_2 and remains there from 40 to 80 min. The inertia constant stays at H_3 during the last 40 min. H_1, H_2 and H_3 can be regarded as the inertia constant vectors here that represent the inertia constant of all generators in different periods.

TABLE 4. Inertia constant of all generators in different periods.

Generator	Bus	H_1 (0-40 min)	H_2 (40-80 min)	H_3 (80-120 min)
G01	39	500	600	400
G02	31	30.3	28	35
G03	32	35.8	32	40
G04	33	28.6	24	36
G05	34	26.0	30	33
G06	35	34.8	40	44
G07	36	26.4	21	31.5
G08	37	24.3	31.5	21
G09	38	34.5	38	42
G10	30	42	36	48

Table 4 shows the inertia constant of all generators in different periods.

All the loads in IEEE 39-bus system are modeled to be random, the same as section IV-B. Then, the inertia constant of all generators in the 39-bus system is tracked using the methods introduced in section III-A to D. The active power output P_i and bus frequency f_i with a 120-min length are measured by PMUs. The sliding window method with a window length of 100 s and a refresh rate of 1 s is employed. For each sliding window, steps 2-4 in section IV-B-1) are employed sequentially and then, the estimates are smoothed using the exponential smoothing method in (17). Once the measurements from the sliding window are obtained, the inertia constant will be estimated immediately. The execution time of a single estimation is less than 1 s, which means that the inertia constant can be updated before new samples are completely collected, leading to real-time online tracking of the inertia constant.

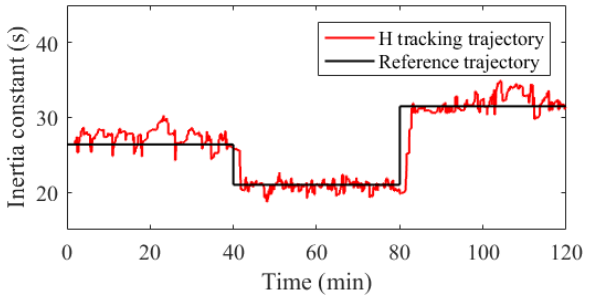

FIGURE 10. Inertia constant tracking trajectory of generator 7.

Inertia constant tracking trajectories of generator 7 and generator 8 are shown in Fig. 10 and Fig. 11, respectively. The inertia constant tracking trajectories of other generators

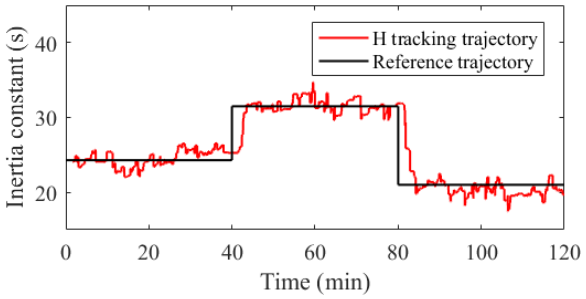

FIGURE 11. Inertia constant tracking trajectory of generator 8.

are not provided here for the limited space. Both Fig. 10 and Fig. 11 show that the inertia constant tracking trajectories fluctuate around the reference trajectories in a small range, meaning that the inertia constant can be tracked accurately in real-time using the proposed method.

According to section III-D, the execution time of the procedures depends on the choice of sliding window length and estimation refresh rate. Table 5 shows the execution time for different settings of sliding window length and refresh rate with a 120-min measurement. The simulations are carried out in a regular office laptop with Inter(R) Core(TM) i7-7700HQ and CPU at 2.80 GHz.

TABLE 5. Execution time for different settings.

Setting	Sliding Window Length (s)	Refresh Rate (s)	Execution Time(s)
1	100	1	2217.55
2	100	2	1075.64
3	100	4	542.35
4	100	5	447.59

The results of the first four settings show that the execution time is inversely proportional to the refresh rate as fewer estimations are done with a slower refresh rate. The execution time of the fifth setting is comparable to the execution time of the first setting, indicating that a larger sliding window length will increase the computational burden. Additionally, processing one measurement period takes approximately 6.22-31.36% of its length using the laptop introduced above. On average, it takes 3.73-18.81 s to analyze 1 min of the measurements. In addition, a sliding window length of 100-200 s with a refresh rate of 1-2 s is responsive enough to obtain reliably accurate results in our simulations.

For various power systems, the sliding window length can be adjusted properly until an acceptable dynamic model can be identified and the faster refresh rated can be determined to track the inertia constant better using a more powerful computer. All the analyses above confirm that the proposed method is suitable for power system inertia constant real-time online tracking.

V. CONCLUSION

This paper proposed an online estimation method for power system inertia constant under normal operating conditions. First, the dynamic model between active power output and bus frequency measured by PMUs was identified using the subspace identification method. Then, the inertia constant was extracted from the unit step response of the identified model in the time domain. Finally, the sliding window method and the exponential smoothing method were used to update the inertia constant in real-time.

The proposed method was tested in the IEEE 39-bus system. The results confirmed that different hierarchical power system inertia constant (individual generator, area and the whole system) could be estimated with high accuracy using ambient data, which could overcome the disadvantages of the disturbance data methods. Moreover, by using the proposed method, the inertia constant could be updated on a time scale of seconds, and the inertia constant tracking trajectories could also be provided in real-time.

REFERENCES

[1] P. Kundur, *Power System Stability and Control*. New York, NY, USA: McGraw-Hill, 1994, pp. 128–136.
[2] V. Gevorgian, Y. Zhang, and E. Ela, "Investigating the impacts of wind generation participation in interconnection frequency response," *IEEE Trans. Sustain. Energy*, vol. 6, no. 3, pp. 1004–1012, Jul. 2015.
[3] S. Eftekharnejad, V. Vittal, G. T. Heydt, B. Keel, and J. Loehr, "Impact of increased penetration of photovoltaic generation on power systems," *IEEE Trans. Power Syst.*, vol. 28, no. 2, pp. 893–901, May 2013.
[4] A. Adrees, P. N. Papadopoulos, and J. V. Milanovic, "A framework to assess the effect of reduction in inertia on system frequency response," in *Proc. IEEE Power Energy Soc. Gen. Meeting (PESGM)*, Jul. 2016, pp. 1–5.
[5] H. Shao, X. Cai, D. Zhou, Z. Li, D. Zheng, Y. Cao, Y. Wang, and F. Rao, "Equivalent modeling and comprehensive evaluation of inertia emulation control strategy for DFIG wind turbine generator," *IEEE Access*, vol. 7, pp. 64798–64811, 2019.
[6] Arani and El-Saadany, "Implementing virtual inertia in DFIG-based wind power generation," *IEEE Trans. Power Syst.*, vol. 28, no. 2, pp. 1373–1384, May 2013.
[7] A. Ghafouri, J. Milimonfared, and G. B. Gharehpetian, "Coordinated control of distributed energy resources and conventional power plants for frequency control of power systems," *IEEE Trans. Smart Grid*, vol. 6, no. 1, pp. 104–114, Jan. 2015.
[8] A. Ulbig, T. S. Borsche, and G. Andersson, "Impact of low rotational inertia on power system stability and operation," *IFAC Proc.*, vol. 47, no. 3, pp. 7279–7290, Dec. 2014.
[9] E. Spahic, D. Varma, G. Beck, G. Kuhn, and V. Hild, "Impact of reduced system inertia on stable power system operation and an overview of possible solutions," in *Proc. IEEE Power Energy Soc. Gen. Meeting (PESGM)*, Jul. 2016, pp. 1–5.
[10] T. Inoue, H. Taniguchi, Y. Ikeguchi, and K. Yoshida, "Estimation of power system inertia constant and capacity of spinning-reserve support generators using measured frequency transients," *IEEE Trans. Power Syst.*, vol. 12, no. 1, pp. 136–143, Feb. 1997.
[11] D. P. Chassin, Z. Huang, M. K. Donnelly, C. Hassler, E. Ramirez, and C. Ray, "Estimation of WECC system inertia using observed frequency transients," *IEEE Trans. Power Syst.*, vol. 20, no. 2, pp. 1190–1192, May 2005.
[12] P. Du and Y. Makarov, "Using disturbance data to monitor primary frequency response for power system interconnections," *IEEE Trans. Power Syst.*, vol. 29, no. 3, pp. 1431–1432, May 2014.
[13] P. M. Ashton, C. S. Saunders, G. A. Taylor, A. M. Carter, and M. E. Bradley, "Inertia estimation of the GB power system using synchrophasor measurements," *IEEE Trans. Power Syst.*, vol. 30, no. 2, pp. 701–709, Mar. 2015.
[14] P. Wall and V. Terzija, "Simultaneous estimation of the time of disturbance and inertia in power systems," *IEEE Trans. Power Del.*, vol. 29, no. 4, pp. 2018–2031, Aug. 2014.
[15] D. Zografos and M. Ghandhari, "Estimation of power system inertia," in *Proc. IEEE Power Energy Soc. Gen. Meeting (PESGM)*, Boston, MA, USA, Jul. 2016, pp. 1–5.

[16] Y. Bian, H. Wyman-Pain, F. Li, R. Bhakar, S. Mishra, and N. P. Padhy, "Demand side contributions for system inertia in the GB power system," *IEEE Trans. Power Syst.*, vol. 33, no. 4, pp. 3521–3530, Jul. 2018.
[17] D. del Giudice and S. Grillo, "Analysis of the sensitivity of the extended Kalman filter based inertia estimation method to the assumed time of disturbance," in *Proc. IEEE Int. Conf. Environ. Electr. Eng. IEEE Ind. Commercial Power Syst. Eur. (EEEIC/I&CPS Europe)*, Palermo, Italy, Jun. 2018, pp. 1–6.
[18] A. Darbandsari, A. Maroufkhani, and T. Amraee, "The estimation of inertia and load damping constants using phasor measurement data," in *Proc. Smart Grid Conf. (SGC)*, Dec. 2017, pp. 1–7.
[19] R. K. Panda, A. Mohapatra, and S. C. Srivastava, "Online estimation of system inertia in a power network utilizing synchrophasor measurements," *IEEE Trans. Power Syst.*, early access, Dec. 9, 2019, doi: 10.1109/TPWRS.2019.2958603.
[20] C. Phurailatpam, Z. H. Rather, B. Bahrani, and S. Doolla, "Measurement based estimation of inertia in AC microgrids," *IEEE Trans. Sustain. Energy*, early access, Oct. 18, 2019, doi: 10.1109/TSTE.2019.2948224.
[21] S. You, Y. Liu, G. Kou, X. Zhang, W. Yao, Y. Su, S. W. Hadley, and Y. Liu, "Non-invasive identification of inertia distribution change in high renewable systems using distribution level PMU," *IEEE Trans. Power Syst.*, vol. 33, no. 1, pp. 1110–1112, Jan. 2018.
[22] X. Cao, B. Stephen, I. F. Abdulhadi, C. D. Booth, and G. M. Burt, "Switching Markov Gaussian models for dynamic power system inertia estimation," *IEEE Trans. Power Syst.*, vol. 31, no. 5, pp. 3394–3403, Sep. 2016.
[23] K. Tuttelberg, J. Kilter, D. Wilson, and K. Uhlen, "Estimation of power system inertia from ambient wide area measurements," *IEEE Trans. Power Syst.*, vol. 33, no. 6, pp. 7249–7257, Nov. 2018.
[24] J. Zhang and H. Xu, "Online identification of power system equivalent inertia constant," *IEEE Trans. Ind. Electron.*, vol. 64, no. 10, pp. 8098–8107, Oct. 2017.
[25] S. D'Arco and J. A. Suul, "Equivalence of virtual synchronous machines and frequency-droops for converter-based MicroGrids," *IEEE Trans. Smart Grid*, vol. 5, no. 1, pp. 394–395, Jan. 2014.
[26] Y. Li, Z. Xu, and K. P. Wong, "Advanced control strategies of PMSG-based wind turbines for system inertia support," *IEEE Trans. Power Syst.*, vol. 32, no. 4, pp. 3027–3037, Jul. 2017.
[27] L. Xiong, F. Zhuo, F. Wang, X. Liu, Y. Chen, M. Zhu, and H. Yi, "Static synchronous generator model: A new perspective to investigate dynamic characteristics and stability issues of grid-tied PWM inverter," *IEEE Trans. Power Electron.*, vol. 31, no. 9, pp. 6264–6280, Sep. 2016.
[28] N. Zhou, J. W. Pierre, and J. F. Hauer, "Initial results in power system identification from injected probing signals using a subspace method," *IEEE Trans. Power Syst.*, vol. 21, no. 3, pp. 1296–1302, Aug. 2006.
[29] J. Zhang and H. Xu, "Microperturbation method for power system online model identification," *IEEE Trans. Ind. Informat.*, vol. 12, no. 3, pp. 1055–1063, Jun. 2016.
[30] S. A. N. Sarmadi and V. Venkatasubramanian, "Electromechanical mode estimation using recursive adaptive stochastic subspace identification," *IEEE Trans. Power Syst.*, vol. 29, no. 1, pp. 349–358, Jan. 2014.
[31] C. Canizares, T. Fernandes, E. Geraldi, L. Gerin-Lajoie, M. Gibbard, I. Hiskens, J. Kersulis, R. Kuiava, L. Lima, F. DeMarco, N. Martins, B. C. Pal, A. Piardi, R. Ramos, J. dos Santos, D. Silva, A. K. Singh, B. Tamimi, and D. Vowles, "Benchmark models for the analysis and control of small-signal oscillatory dynamics in power systems," *IEEE Trans. Power Syst.*, vol. 32, no. 1, pp. 715–722, Jan. 2017.
[32] N. Ma and D. Wang, "Extracting spatial-temporal characteristics of frequency dynamic in large-scale power grids," *IEEE Trans. Power Syst.*, vol. 34, no. 4, pp. 2654–2662, Jul. 2019.

FANHONG ZENG (Graduate Student Member, IEEE) was born in Guangdong, China, in March 1994. He received the B.Eng. degree in electrical engineering from the School of Electric Power, South China University of Technology, in 2017, where he is currently pursuing the M.Eng. degree. His research interests include power system stability and control, system identification, and power system inertia estimation.

JUNBO ZHANG (Senior Member, IEEE) received the B.S. and Ph.D. degrees in electrical engineering from Tsinghua University, in 2008 and 2013, respectively. He visited The Hong Kong Polytechnic University and Stanford University, from 2009 to 2010 and from 2018 to 2019, respectively. He is currently a Professor with the School of Electric Power Engineering, South China University of Technology. His research areas include artificial intelligent and hyper-automatics in complex system operation and decision making, knowledge-based expert systems with distributed cloud computing, power system simulation with high-performance parallel computing, and power system operation and control.

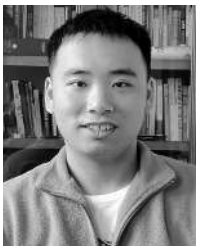

GE CHEN (Graduate Student Member, IEEE) was born in Guangdong, China, in November 1995. He received the bachelor's degree in electrical engineering from the School of Electric Power Engineering, South China University of Technology, in 2018, where he is currently pursuing the M.Eng. degree in electrical engineering. His research interests include power system dispatch and application of artificial intelligence in smart grids.

ZIKUN WU was born in Guangdong, China, in February 1996. He received the B.Eng. degree in electrical engineering from the School of Electric Power, South China University of Technology, in 2019, where he is currently pursuing the M.Eng. degree in electrical engineering. His research interests include power system modeling, simulation and analysis, and software architecture in power systems.

SIWEI HUANG was born in Shanxi, China, in October 1994. She received the B.Eng. degree in electrical engineering from Hehai University, in 2017. She is currently pursuing the M.Eng. degree in electrical engineering with the South China University of Technology. Her research interests include system identification and power system inertia estimation, and application of artificial intelligence algorithms in power systems.

YINGQI LIANG (Member, IEEE) received the B.Eng. degree in electrical engineering from the South China University of Technology. She is currently pursuing the Ph.D. degree in electrical and computer engineering with the National University of Singapore. Her research interests include in the learning, optimization, and control of networked cyber-physical systems, with particular applications to power systems.